# Ab initio calculations of electronic interactions in inclusion complexes of calix- and thiacalix[n]arenes and block s cations

**3 AUTHORS:**

Joaquin Barroso-Flores
Universidad Nacional Autónoma de México
**19** PUBLICATIONS **78** CITATIONS

SEE PROFILE

Petronela M. Petrar
Babeş-Bolyai University
**32** PUBLICATIONS **63** CITATIONS

SEE PROFILE

Sándor Kunsági-Máté
University of Pécs
**97** PUBLICATIONS **727** CITATIONS

SEE PROFILE

ORIGINAL ARTICLE

# Ab initio calculations of electronic interactions in inclusion complexes of calix- and thiacalix[*n*]arenes and block *s* cations

Joaquín Barroso-Flores · Ioan Silaghi-Dumitrescu ·
Petronela M. Petrar · Sándor Kunsági-Máté

**Abstract** Ab initio calculations at the HF/6-31G(*d*) level of theory were performed on a series of thiacalix[4]arenes and calix[6]arenes in presence and in absence of monovalent (Li$^+$, Na$^+$ and Cs$^+$) and divalent cations (Ca$^{2+}$ and Ba$^{2+}$) respectively, in order to evaluate their particular bonding properties as host systems towards electrically charged species. NBO, as well as NBO deletion calculations were undertaken to evaluate the energy difference in the circular hydrogen bonding at the lower rim once an ion was placed inside the cavity. Disruption of this H-bonded system is dependent on the position of the ion within the guest and not on its ionic ratio. The basis set superposition error and the NBO deletion energy between the host and guest species were calculated in order to assess the interaction energy between them.

J. Barroso-Flores · I. Silaghi-Dumitrescu · P. M. Petrar
Faculty of Chemistry and Chemical Engineering, Babes-Bolyai University, 11, Arany Janos Str., 400028 Cluj-Napoca, Romania

J. Barroso-Flores · S. Kunsági-Máté (✉)
Department of General and Physical Chemistry,
University of Pécs Ifjúság, 6, Pécs 7624, Hungary
e-mail: kunsagi@gamma.ttk.pte.hu

J. Barroso-Flores
Centro Conjunto de Investigación en Química Sustentable
UAEM–UNAM, Carretera Toluca-Atlacomulco km 14.5,
Unidad San Cayetano, Toluca, Estado de México,
50200 Mexico, Mexico

S. Kunsági-Máté
Janos Szentagothai Research Center,
34 Ifjusag Str., Pecs 7624, Hungary

## Introduction

The realm of molecular recognition is based on the control of specific interactions between two or more chemical species; such interactions range from van der Waals interactions to electrostatic ones and chemical bonding, including coordination bonds. The use of macrocycles as hosts to form inclusion complexes is one of the many strategies employed for the purpose of selectively trap different chemical species; some kinds of these macrocycles include crown ethers, cyclodextrins and calixarenes. Calix[*n*]arenes are a family of bowl or cone shaped macrocycles synthesized through the condensation of phenol derivatives with an aldehyde [1, 2], which in recent times have known a growing interest as far as their hosting properties as molecular recognition agents are concerned [3–9]. This is because these molecules have very wide application in sensor chemistry, they are applied in electrochemical [10] or fluorescent sensors [11] and sensing potential ranges from toxic metals [12] to proteins [13]. They also play a considerable role as carrier molecules extracting ionic media to nonpolar solvents and otherwise thus improving the solubility of nonpolar species into aqueous or other solutions having high permittivity [14, 15].

In our recent works we have shown that the flexibility of the skeleton of host molecules affects significantly the stability of host–guest complexes [16]. This is because the inclusion of the guest molecules usually associated with the change of the conformation of the host and the flexibility of the host skeleton also changed by the formation of the complex. This effect highly depends on the coordination site of the guest species towards the host skeleton. We also have shown previously that the charge of the guest iron ion have determinant role according to the site

of coordination to the host's skeleton [17] and the coordination site of the metal ions affects the complexation ability of host towards neutral species [18]. As one possible approximation, chemical reactivity principles of electronegativity and chemical hardness have been applied recently to describe the affinity towards guests at molecular level [19–21].

Due to the flexibility of the macrocyclic backbone, which becomes larger with the number of phenol units involved in its formation, several conformations are possible to be attained; in the specific case of a generic calix[4]arene, four major distinct conformers are observed, namely cone, partial cone, 1,2-alternate and 1,3-alternate [22]. Such conformers are shown in Fig. 1. The number of available conformers increases with the size of the macrocycle, providing a larger flexibility towards guests of various sizes, which in turn may serve as scaffolds or templates to stabilize the host in a given conformation according to the major interactions in role.

Specific affinity of these macrocycles may be tuned through proper selection of functional groups attached to the upper rim as well as by modifying their size, controlling thus the specific interactions between host and guests. In this regard, theoretical calculations help designing appropriate calixarene skeletons by computing the specific values of different classes of interactions between them and potential guest molecules. In this work we intend to shed light on the electronic properties of calixarenes towards the inclusion of different cations in their cavities.

## Computational methods

All calculations were performed with the Gaussian03 Rev. D.02 [23] suite of programs at the HF/6-31G($d$) level of theory. NBO and NBODel calculations were carried out with the NBO3.1 program [24] as included in the aforementioned Gaussian package.

Upper rim sulfonato-functionalized calixarenes and thiacalixarenes were considered; two sizes were employed throughout this study: {$n = 4, 6$}. With the former, Li$^+$, Na$^+$ and Cs$^+$ ions were used as guest species whereas with the latter Ca$^{2+}$ and Ba$^{2+}$ were employed. The purpose of such selection was to evaluate the different scenarios in which an ion could lie on the lower rim, inside the cavity and on the upper rim depending on the chemical environment in each of these regions.

## Results

Geometry optimization calculations at the RHF/6-31G($d$) level of theory were performed on all compounds. In the case of compounds (**3**), (**4**) and (**5**) (M = Cs$^+$, Ca$^{2+}$ and Ba$^{2+}$) the Hay and Wadt [25] pseudopotential along with its corresponding basis set was employed on the metallic ion. Vibrational analyses were then undertaken in order to ascertain that the obtained structures corresponded to minima on their respective potential energy surfaces. No imaginary frequencies were observed. Figure 2a recollects the optimized structures of free hosts while Fig. 2b shows



**Fig. 1** Four main conformers exhibited by calix[4]arene: **a** cone, **b** partial cone, **c** 1,2-alternate, **d** 1,3-alternate
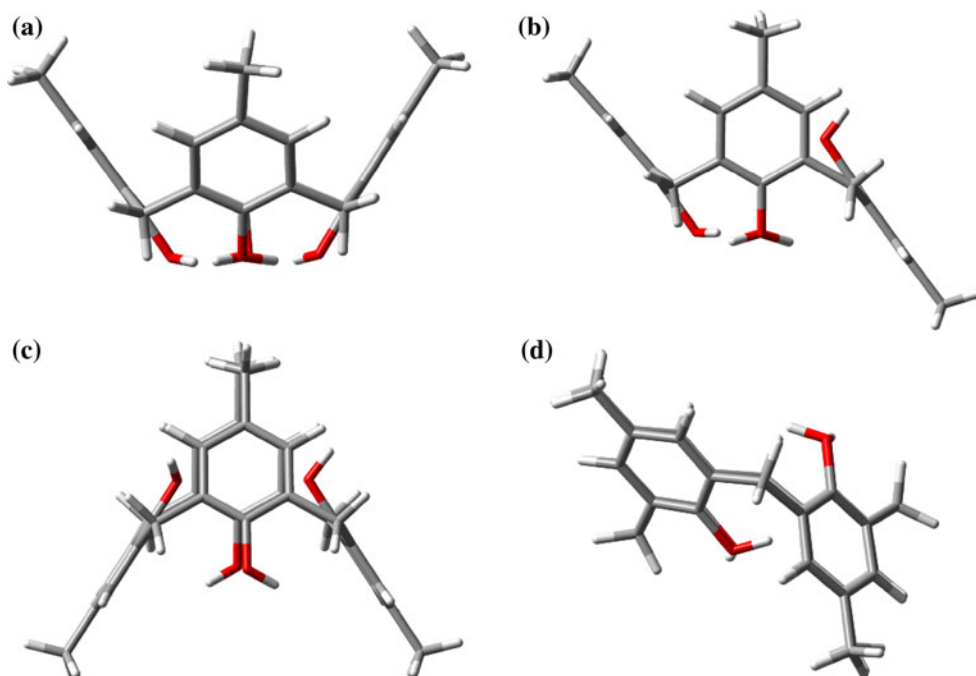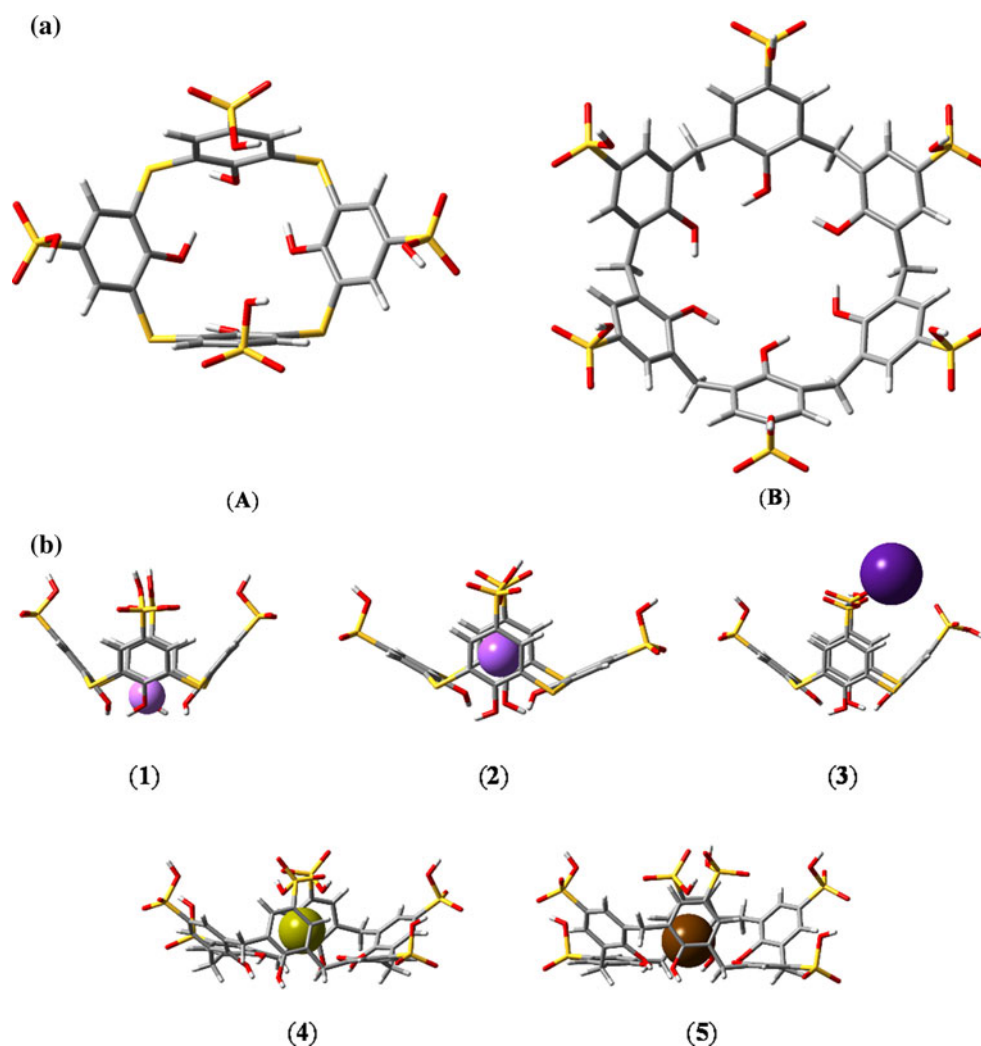
**Fig. 2** **a** Optimized geometries for the free hosts. **b** Optimized geometries for compounds (**1**) through (**5**) at the RHF/6-31G(*d*) level of theory



those of the formed inclusion compounds (**1**) through (**5**). Upon inclusion of the ionic guest the common circular Hydrogen bonding on the lower rim in the case of calix[4] is preserved, whereas in the case of calix[6] it is lost due to the transition to a conformation which could be described as intermediate between cone and 1,4-alternate; phenol units 1 and 4 become almost coplanar due to the H bonding between units 3 and 6 through the SO$_3$H groups on the upper rim.

In cases where possible, the skeleton of the calixarene host molecule formed intramolecular hydrogen bonds between the sulfonato moieties located on the upper rim. Such is the case of compound (**1**) (M = Na$^+$) complex in which it is possible to observe how the formation of a hydrogen bond between two sulfonato moieties opposite each other across the upper rim closes the cavity of the host molecule on the ion keeping it trapped in a pocket fashion. This feature along with the cavity-ionic radius ratio will allow us to design host molecules with an enhanced capability of sequestering ions based on the relative size

ratio (fitting) of the host–guest system and the possibility of strong electronic interactions across the upper rim which keep the ions trapped. The same hydrogen bond locking effect across the upper rim is observed for compounds (**4**) and (**5**) for which the regular geometry of the cone conformation (C$_6$ point group) is lost upon inclusion of the alkaline earth cation. The clasping of the guest by the host yields the geometry of the latter best described as a pressed cone.

In order to evaluate the necessary energy to switch the hydrogen bonding in the lower rim three different PES scans were calculated, with and without a cation inside the cavity: A rigid scan in which the equilibrium structure of the host (**A**) was used as a starting point, dihedral angles (see Scheme 1 for numbering) C22–C23–O3–H39; C14–C15–O2–H38; C7–C6–O1–H40 and C30–C31–O4–H5 were simultaneously varied by 20° increments starting from their original values until reaching a structure similar to the corresponding enantiomer without allowing for any other variable to be optimized (a); a fully relaxed scan (all
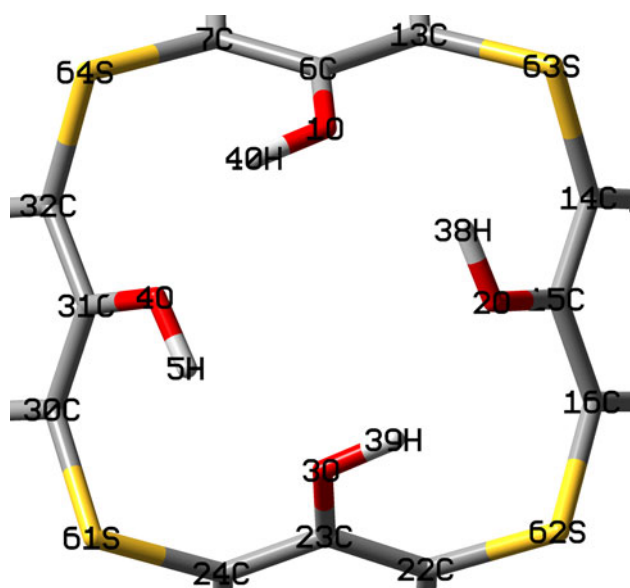
**Scheme 1** Numbering system for host (**a**). Only the lower rim view is shown for clarity

variables were optimized at each step) in which the same incremental procedure as in (a) was employed; and a partially relaxed scan for which the dihedral angles were kept frozen at every step but all the other variables were optimized at each step (c). Both in (b) and (c) procedures the obtained structure of each step was used as input for the following one. The computed values for all energy barriers calculated are summarized in Table 1.

Figure 3 shows the energy profile along the scan for all three procedures performed on host (**A**). In the case of the fully relaxed scan, the structure keeps on returning to the original equilibrium geometry, hence the short or negligible change in energy from one step to the next, until the near 90.0° point is reached. At this point, all H atoms in the lower rim are pointing towards the center of the lower rim. In all subsequent steps the structure reaches the geometry of the enantiomer and once again keeps on falling to the equilibrium geometry with the complete circular H bonding.

Both the fully rigid and the partially relaxed scans exhibit a normal distribution with energy barriers of

**Table 1** Energy barriers for circular H bonding inversion in lower rim

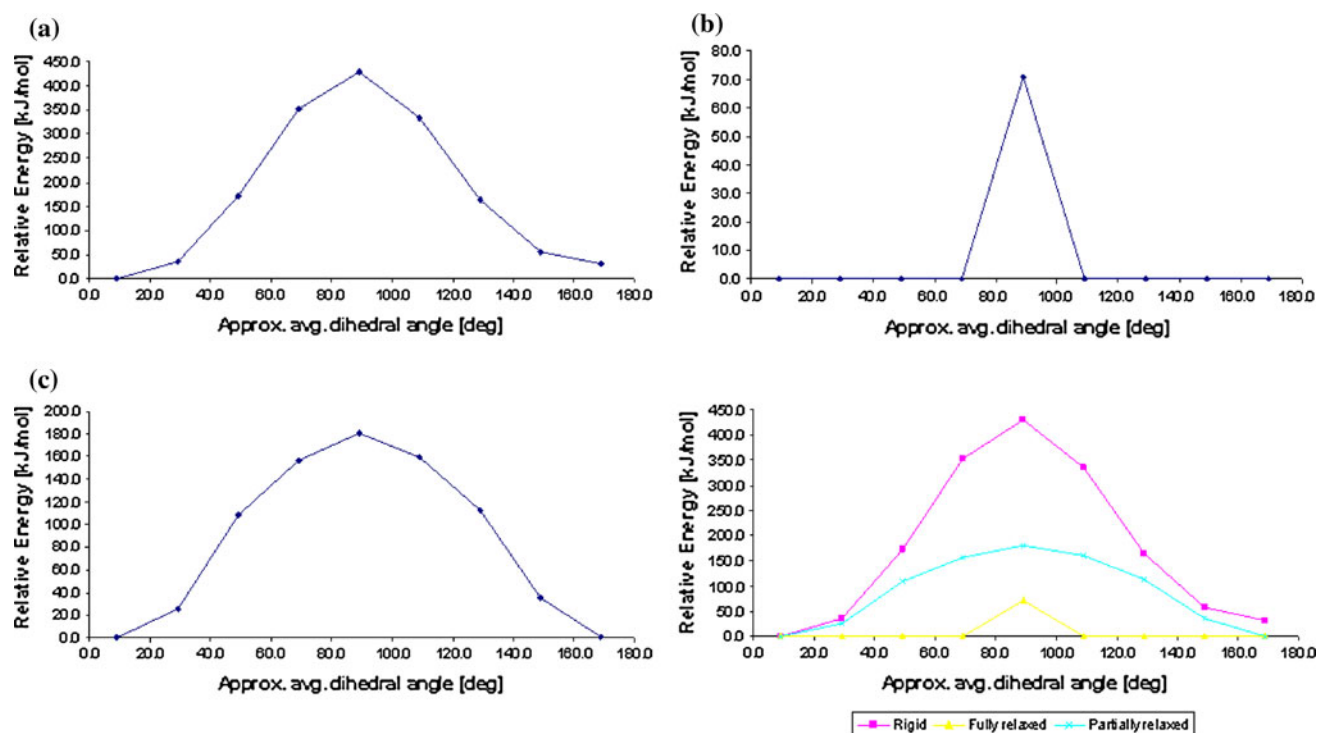| Procedure for the PES scan | Rigid (a) | Fully relaxed (b) | Partially relaxed (c) |
|---|---|---|---|
| Energy barrier [kJ/mol] | 429.3578 | 70.7834 | 180.9034 |



**Fig. 3** Plots for the energy barrier scan in the circular H bonding inversion of (**1**) **a** Rigid scan. Only dihedral angles under study are changed at every step; **b** fully relaxed scan. At every step all variables are optimized; **c** partially relaxed scan. Dihedral angles under study were kept frozen at each point while the rest of the variables were optimized; **d** all three scans are shown together for comparison

429.3578 and 180.9034 kJ/mol, respectively. The latter is lower since the system is allowed to relax and the angle between planes changes continuously throughout the process. Furthermore, two sulfonato groups directly across from each other on the upper rim form a hydrogen bond which accounts for some stabilization of those states close to the energy maximum. At this stage of the scan two phenol units become almost parallel allowing for the formation of the intramolecular Hydrogen bond which in turn stabilizes the intermediate conformation. In Fig. 4 the change of the interplanar angle between opposite aromatic rings along the PES scan is shown. Such angles are labeled as alpha and beta according to Scheme 2. In this plot we observe how the cone shape, in a near C4 symmetry, is broken into C2 when reaching the fourth step of the scan. Starting with the fourth point, rings 2 and 4 remain practically parallel due to the hydrogen bond formed between their corresponding sulfonato groups. Rings 1 and 3 push the skeleton back into a near C4 symmetry by closing the plane angle between them.

The presence of these hydrogen bonding groups across the molecule offers a clamping effect that keeps the guest inside the cavity as discussed earlier. Figure 5 provides a closer view of compound (1).
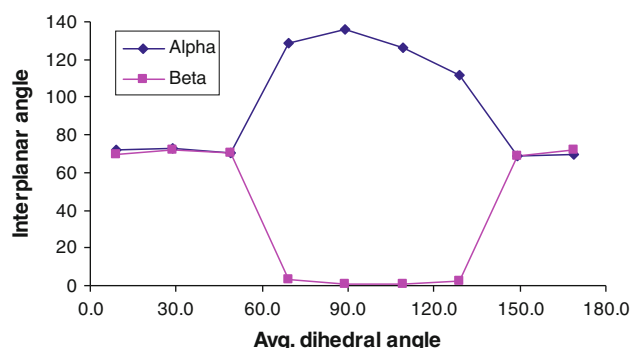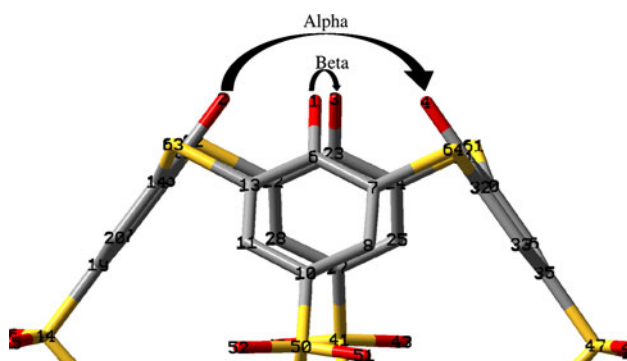


**Fig. 4** Change in interplanar angle during H bonding PES scan



**Scheme 2** Numbering scheme for dihedral angle measurements (hydrogen atoms are omitted for clarity)

In Fig. 6 the molecular electrostatic potential (MEP) is mapped upon the electron density calculated at the HF/6-31G($d$, $p$) level of theory for both hosts (**A**) and (**B**), respectively. Therein it is possible to observe that the aromatic rings that form both cavities have different values of MEP despite having the same composition. In host (**A**) the electrostatic potential around the aromatic rings has a value close to $-0.04$ esu while in host (**B**) the value is closer to $-0.05$ esu. The larger macrocycle is thus slightly more nucleophilic than the smaller one.

The sulfur atoms located on the upper rim substituents in host (**A**) exhibit a more negative potential than their corresponding counterparts in host (**B**), thus giving the smaller host (**A**) a higher affinity towards coordinating ionic species through the upper rim which in turn might lead to a higher recognition capability.

NBO and NBO deletion computations were employed to evaluate the bonding properties of the circular hydrogen bonding system present in the lower rim of host (**A**). Table 2 shows the energy change when the H···O elements are deleted from the Fock matrix and this is once again diagonalized. Only host (**A**) was included in this part of the study due to the larger flexibility of host (**B**) and its consequent lost of the circular H-bond upon complex formation.

In order to assess the influence of the ion in the disruption of the hydrogen bonding at the lower rim we also performed the same deletion analysis on the equilibrium geometries of the complexes but without the ion, which was simply removed from the structure. The values for these calculations are included in Table 3 along with the energy change values in presence of the ion for the same equilibrium geometry.

Since the Cs$^+$ ion lies on the upper rim on account of its large size compared to the internal diameter of the host cavity, its influence on the H bonding at the lower rim is much lower than in the other two cases; the large difference in H bonding energy for the parent calixarene and the Cs$^+$ complex (127.9878 and 45.3660 kJ/mol, respectively) is due to the conformational change in the host molecule,
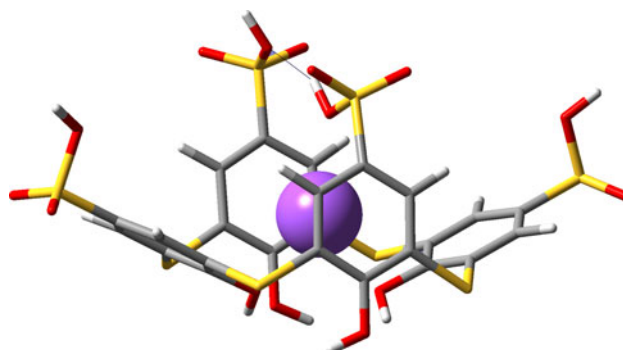


**Fig. 5** Optimized structure for compound (**2**). The Na$^+$ cation is trapped inside the thiacalix[4]arene tetrasulfonate cavity pocket
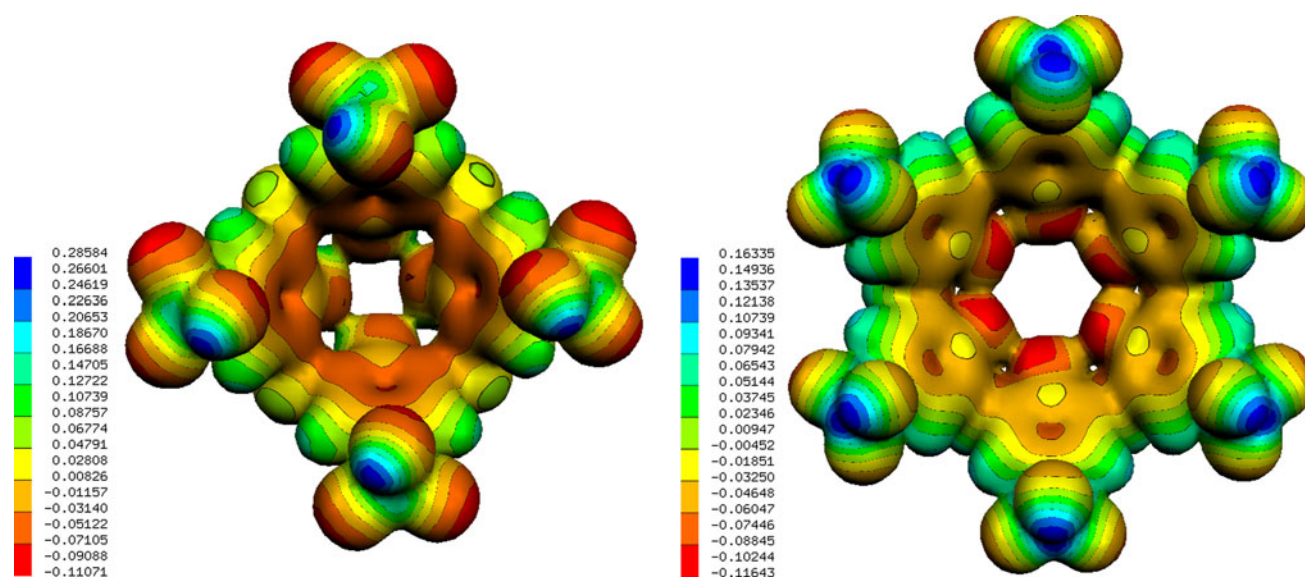
**Fig. 6** Molecular electrostatic Potential mapped onto the electron density calculated at the HF/6-31G($d$, $p$) level of theory. Electron density plotted at the 0.02 e/Å$^3$ isosurface value

**Table 2** Energy change upon deletion of all interactions concerning the circular H bonding at the lower rim

| Ion inside the cavity | Energy change (kJ/mol) |
|---|---|
| None | 127.9878 |
| Li$^+$ | 11.6835 |
| Na$^+$ | 16.8846 |
| Cs$^+$ | 45.3660 |

**Table 3** Energy change upon deletion of all interactions concerning the circular H bonding on the lower rim in the absence of the ion

| Ion in host (a) | Energy change with ion (kJ/mol) | Energy change without the ion (kJ/mol) | Change (%) |
|---|---|---|---|
| Li$^+$ | 11.6835 | 15.4458 | 32.20 |
| Na$^+$ | 16.8846 | 20.7887 | 23.12 |
| Cs$^+$ | 45.3660 | 47.3903 | 4.46 |



**Fig. 7** Optimized structure for compound (**1**). The Li$^+$ cation lies closer to the lower rim disrupting the circular H-bond system by means of reorienting the lone pairs on oxygen atoms

**Table 4** BSSE corrections to total energy for compounds (**1**) through (**5**) (kJ/mol)

| Compound | (**1**) | (**2**) | (**3**) | (**4**) | (**5**) |
|---|---|---|---|---|---|
| Ion | Li$^+$ | Na$^+$ | Cs$^+$ | Ca$^{2+}$ | Ba$^{2+}$ |
| BSSE energy | 18.5320 | 19.5921 | 9.6614 | 25.7551 | 23.6198 |

deviating from C4 to a near C2 symmetry. In the case of the Li$^+$ complex, compound (**1**), the circular H bonding is almost lost, which can be observed by the change in the relative orientation of the OH bonds towards their neighboring OH groups (See Fig. 7), which is not collinear as in the case of the free host. Complexation of the Li$^+$ ion is performed through the O electron lone pairs; a similar effect is observed to a lesser extent in the Na$^+$ complex due to the location of the ion closer to the center of the cavity.

In order to further assess the bonding strength between the host and guest species we calculated the basis set superposition error (BSSE) through the counterpoise method [26, 27]. Values for the energy correction obtained at the optimized conformations are presented in Table 4.
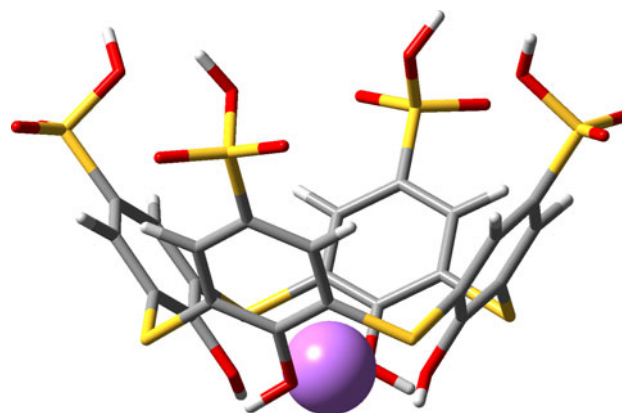
BSSE values for compounds (**1**) and (**2**) are close to each other, which suggest that the orbital part of host–guest interactions is not dependent of the location of the ion within the cavity, which in turn suggests that the electrostatic part of the interaction governs the formation of the complex. The same reasoning is employed for the values obtained for compounds (**4**) and (**5**), although a larger

difference is observed than in the previous case despite a higher similarity between their conformations and the relative positions of the ions within their respective cavity. The value for compound (**3**) differs from the corresponding ones for (**1**) and (**2**) due to the presence of the pseudopotential.

For comparison, the total deletion energy between host and guest were computed for compounds (**1**) and (**2**). The change in energy for the former is 527.263 kJ/mol while for the latter the obtained value is 1110.906 kJ/mol.

## Conclusions

Hydrogen bonding in the lower rim of calixarenes becomes disrupted by the presence of a small or medium sized cation in the cavity. Large cations lying on the upper rim disrupt the H bonding system by means of general structure distortion of the skeleton on the guest molecule but not by means of direct bonding interactions with the corresponding OH groups in the lower rim. Thus, not only the charge in a charge-dipolar interaction, but also fitting of the cation within the cavity is essential for optimizing the interactions between host and guest.

The presence of hydrogen bond donor/acceptor functional groups at the upper rim allows the host to stabilize the closed-pocket conformations as seen in compounds (**1**), (**4**) and (**5**), giving the hosts the ability of closely trapping ions within their cavities. The nucleophilicity of the upper rim substituents, as well as that of the aromatic groups forming the cavity can be increased by decreasing the size of the ring at the expense of the size fitting component of the inclusion process.

Similar BSSE values for compounds (**1**) and (**2**) suggest the ionic ratio is of little importance in the total interaction energy which in turn suggests a stronger electrostatic contribution. The same reasoning can be applied to the low difference observed between compounds (**4**) and (**5**) whereas compound (**3**) has a lower BSSE value given the fact that it lies almost completely outside the macrocycle.

## References

1. Redshaw, C.: Coordination chemistry of the larger calixarenes. Coord. Chem. Rev. **244**, 45–70 (2003)
2. Śliwa, W.: Calixarene complexes with transition metal ions. J. Incl. Phenom. Macrocycl. Chem. **52**, 13–37 (2005)
3. Mutihac, L., Lee, J.H., Kim, J.S., Vicens, J.: Recognition of amino acids by functionalized calixarenes. Chem. Soc. Rev. **40**, 2777–2796 (2011)
4. Branco, T.J.F., Ferreira, L.F.V., do Rego, A.M.B., Oliveira, A.S., Da Silva, J.P.: Pyrene–p-tert-butylcalixarenes inclusion complexes formation: a surface photochemistry study. Photochem. Photobiol. Sci. **5**, 1068–1077 (2006)
5. Coquiere, D., de la Lande, A., Marti, S., Parisel, O., Prange, T., Reinaud, O.: Molecular recognition and self-assembly special feature: multipoint molecular recognition within a calix[6]arene funnel complex. Proc. Natl. Acad. Sci. USA **106**, 10449–10454 (2009)
6. Kim, S.J., Kim, B.H.: Syntheses and structural studies of calix[4]arene–nucleoside and calix[4]arene–oligonucleotide hybrids. Nucleic Acids Res. **31**, 2725–2734 (2003)
7. Giria, N.G., Chauhana, S.M.S.: Spectroscopic and spectrometric studies of anion recognition with calix[4]pyrroles in different reaction conditions. Spectrochim. Acta **74**, 297–304 (2009)
8. Joseph, R., Chinta, J.P., Rao, C.P.: Benzothiazole appended lower rim 1,3-di-amido-derivative of calix[4]arene: synthesis, structure, receptor properties towards $Cu^{2+}$, iodide recognition and computational modelling. Inorg. Chim. Acta **363**, 2833–2839 (2010)
9. Peng, Q., Tanga, X.H.: Synthesis of a novel calix[4]arene-based fluorescent ionophore and its metal ions recognition properties. Chin. Chem. Lett. **20**, 13–16 (2009)
10. El Nashar, R.M., Wagdy, H.A.A., Aboul-Enein, H.Y.: Applications of calixarenes as potential ionophores for electrochemical sensors. Curr. Anal. Chem. **5**(3), 249–270 (2009)
11. Kim, J.S., Quang, D.T.: Calixarene-derived fluorescent probes. Chem. Rev. **107**(9), 3780–3799 (2007)
12. Leray, I., Valeur, B.: Calixarene-based fluorescent molecular sensors for toxic metals. Eur. J. Inorg. Chem. **24**, 3525–3535 (2009)
13. Coleman, A.W., Perret, F., Moussa, A., Dupin, M., Guo, Y., Perron, H.: Calix[n]arenes as proteins sensors. Topics Curr. Chem. **277**, 31–88 (2007)
14. Kunsági-Máté, S., Szabó, K., Bitter, I., Nagy, G., Kollár, L.: Complex formation between water-soluble sulfonated calixarenes and C60 fullerene. Tetrahedron Lett. **45**(7), 1387–1390 (2004)
15. Kunsági-Máté, S., Vasapollo, G., Szabó, K., Bitter, I., Mele, G., Longo, L., Kollár, L.: Effect of covalent functionalization of C60 fullerene on its encapsulation by water soluble calixarenes. J. Incl. Phenom. Macrocycl. Chem. **60**(1–2), 71–78 (2008)
16. Kunsági-Máté, S., Csók, Zs., Iwata, K., Szász, E., Kollár, L.: Permittivity-dependent entropy driven complexation ability of cone and paco tetranitro-calix[4]arene toward para-substituted phenols. J. Phys. Chem. B **115**, 3339–3343 (2011)
17. Kunsági-Máté, S., Nagy, L., Nagy, G., Bitter, I., Kollár, L.: Complex formation of Fe(II) and Fe(III) ions with octafunctionalized C-methyl-calix[4]resorcinarene possessing –OCH₂COOH (K) moieties. J. Phys. Chem. B **107**, 4727–4731 (2003)
18. Kunsági-Máté, S., Szabó, K., Lemli, B., Bitter, I., Nagy, G., Kollár, L.: Increased complexation ability of water-soluble calix[4]resorcinarene octacarboxylate towards phenol by the assistance of Fe(II) ions. J. Phys. Chem. B **108**(40), 15519–15524 (2004)
19. Putz, M.V., Russo, N., Sicilia, E.: On the application of the HSAB principle through the use of improved computational schemes for chemical hardness evaluation. J. Comput. Chem. **25**, 994–1003 (2004)
20. Putz, M.V.: On absolute aromaticity within electronegativity and chemical hardness reactivity pictures. Commun. Math. Comput. Chem. **64**, 391–418 (2010)
21. Putz, M.V.: Maximum hardness index of quantum acid-base bonding. Commun. Math. Comput. Chem. **60**, 845–868 (2008)
22. Hong, J., Ham, S.: Comparative study of calix[4]arene derivatives: implications for ligand design. Tetrahedron Lett. **49**, 2386–2393 (2008)

23. Frisch, M.J., Trucks, G.W., Schlegel, H.B., Scuseria, G.E., Robb, M.A., Cheeseman, J.R., Montgomery Jr., J.A., Vreven, T., Kudin, K.N., Burant, J.C., Millam, J.M., Iyengar, S.S., Tomasi, J., Barone, V., Mennucci, B., Cossi, M., Scalmani, G., Rega, N., Petersson, G.A., Nakatsuji, H., Hada, M., Ehara, M., Toyota, K., Fukuda, R., Hasegawa, J., Ishida, M., Nakajima, T., Honda, Y., Kitao, O., Nakai, H., Klene, M., Li, X., Knox, J.E., Hratchian, H.P., Cross, J.B., Adamo, C., Jaramillo, J., Gomperts, R., Stratmann, R.E., Yazyev, O., Austin, A.J., Cammi, R., Pomelli, C., Ochterski, J.W., Ayala, P.Y., Morokuma, K., Voth, G.A., Salvador, P., Dannenberg, J.J., Zakrzewski, V.G., Dapprich, S., Daniels, A.D., Strain, M.C., Farkas, O., Malick, D.K., Rabuck, A.D., Raghavachari, K., Foresman, J.B., Ortiz, J.V., Cui, Q., Baboul, A.G., Clifford, S., Cioslowski, J., Stefanov, B.B., Liu, G., Liashenko, A., Piskorz, P., Komaromi, I., Martin, R.L., Fox, D.J., Keith, T., Al-Laham, M.A., Peng, C.Y., Nanayakkara, A., Challacombe, M., Gill, P.M.W., Johnson, B., Chen, W., Wong, M.W., Gonzalez, C., Pople, J.A.: Gaussian 03, Revision B.02. Gaussian Inc., Pittsburgh, PA (2003)

24. Glendening, E.D., Reed, A.E., Carpenter, J.E., Weinhold, F.: Natural bond orbital/natural population analysis/natural localized molecular orbital program package. NBO Version 3.1 (2003)

25. Hay, P.J., Wadt, W.R.: Ab initio effective core potentials for molecular calculations. Potentials for K to Au including the outermost core orbitals. J. Chem. Phys. **82**, 299–310 (1985)

26. Boys, S.F., Bernardi, F.: Calculation of small molecular interactions by differences of separate total energies: some procedures with reduced errors. Mol. Phys. **19**, 553–566 (1970)

27. Simon, S., Duran, M., Dannenberg, J.J.: How does basis set superposition error change the potential surfaces for hydrogen-bonded dymers. J. Chem. Phys. **105**(1996), 11024–11031 (1031)